Proceedings of the ASME 2023 18th International Manufacturing Science and Engineering Conference
MSEC2023
June 12-16, 2023, New Brunswick, New Jersey

MSEC2023-104321

AN INVESTIGATION ON 3D BIO-PRINTED SCAFFOLD SHAPE FIDELITY INCUBATED IN A CUSTOM-MADE PERFUSION BIOREACTOR

Jack Mankowsky
Department of Sustainable Product Design and Architecture, Keene State College, Keene, NH.

Connor Quigley
Department of Sustainable Product Design and Architecture, Keene State College, Keene, NH.

Scott Clark
Department of Sustainable Product Design and Architecture, Keene State College, Keene, NH.

MD Ahasan Habib*
Department of Sustainable Product Design and Architecture, Keene State College, Keene, NH.

ABSTRACT

Three-dimensional (3D) bioprinting is a promising technique for creating patient-specific 3D scaffolds of tissues or organs. An appropriate culturing process is critical to confirm encapsulated and seeded cells' excellent viability and proliferation into scaffolds materials. Traditional stagnant cell culturing methods don't ensure entering medium inside areas or passing through the scaffolds. To resolve this issue, we developed a customized perfusion bioreactor to supply the growth medium dynamically to the encapsulated or seeded cells. Our custom-designed bioreactor improves the in vivo stimuli and conditions, which may enhance cell viability and proliferation performance. A design of a dual medium tank was utilized allowing the replacement of already-used medium without interrupting perfusion. Accommodating an array of cassettes in a newly designed perfusion chamber allowed a wide range of scaffolds with various size and shapers to hold. In this paper, we explored fluid flow response on scaffolds fabricated with various material compositions with different viscosities. We fabricated scaffolds following a 0^0*-*90^0 *deposition pattern with 8% Alginate, 4% Alginate-4% Carboxymethyl Cellulose (CMC), and 2% Alginate-6% CMC incubated, allowing a constant fluid flow for various periods such as 1, 2, 4, and 8 hours. The change of scaffolds fabricated with multiple material compositions was determined in terms of swelling rate, i.e., change of filament width, and material diffusion, i.e., comparison of dry material weight before and after incubation. This comparative study can assist in application-based materials selection suitable for incubating in a perfusion bioreactor.*

1. INTRODUCTION

Three dimensional (3D) scaffolds fabricated with targeted materials using different techniques may simulate the complex extracellular matrix (ECM) components and structures of native tissue microenvironment that may not be feasible for 2D counterparts. Therefore, 3D scaffolds often build a bridge between 2D level research and animal experiments [1]. 3D scaffolds are frequently used in tissue engineering that intends the organs or tissues regeneration artificially to replace damaged or sick ones in the human body. Enormous potentials of tissue engineering aims to overcome the challenges of existing organ shortage and transplantation requirements [2]. A set of essential steps involved for a successful tissue engineering such as cell extraction, cell incubation and proliferation by 2D culture, fabrication of engineered scaffold, cell maturation in scaffold i.e., tissue generation, and implementation. Improper selection of cell culture technique can hinder the required supply of nutrition to support cell growth and tissue maturation [3] where bioreactor can play an important role to expedite cell growth providing fresh growth factors dynamically [4, 5]. Among various bioreactors, perfusion one can supply fresh nutrient axially through 3D scaffolds including all-natural stimuli that have an impact on cell growth and differentiation [4]. However, existing perfusion bioreactors have issues such as designed around a specific cellular scaffold which limits their function in terms of varied or long-term research [4, 5].

Recently we designed and manufactured a customized perfusion-based bioreactor for culturing 3D bio-printed scaffolds [6]. Our proposed perfusion bioreactor is a Dual Tank, Multichambered, Cellular scaffold incubation unit designed to incorporate both Pressure modulation, and Scaffold Customizability. This is to say our Bioreactor can be used for culturing more than one specific type of 3-dimensional scaffold. The Bioreactor is comprised of four modules each playing a part, either alone or in tandem, mimicking in-vivo conditions. These modules are as follows: the perfusion chambers, the medium tanks, the waste port, the perfusion pump. This Bioreactor was created to aid in the research of 3-dimensional scaffolds capable of supporting cells. An overview of our proposed bioreactor architecture is shown in Figure 1.

Some works have been reported where scaffolds were incubated in perfusion bioreactor and reported positive impact on cell growth [7-9]. In one research, perfused scaffolds fabricated with HA-PLG exhibited increased DNA content and expression of osteogenic markers up to 14 days in culture that plateaued thereafter compared to scaffolds incubated culture placed on shaker. Moreover, hMSC showed a persistent increment of neovascularization in scaffolds cultured under perfusion for 7 days relative to those cultured for 1 day [10].

Recently, MC3T3-E1 murine preosteoblastic cells were seeded into scaffold fabricated with PLGA and nHA compositions and incubated into perfusion bioreactor which showed better cell proliferation compared to static culture [11]. However, the material used in both works were not soft hydrogel. A bioreactor chamber was designed and analyzed for a combination of bidirectional perfusion and electrical stimulation and monitored the Matrigel scaffold functionality without interrupting the culture [12]. With an intention to fabricate bone tissue, hMSC cells were seeded into Dexamethasone-Loaded Peptide Hydrogel and incubated in perfusion bioreactor [13]. The scaffolds used in [12, 13] was not 3D bioprinted. To fabricate scaffold having open channels with Photopolymerizable polyethylene glycol-based hydrogel, stereolithography (SLA) was employed and perfused culture. SLA process parameters were analyzed to maximize the cell viability [14]. However, the pore closure rate incubated into perfusion bioreactor was not analyzed in this paper.

Many studies have shown that creating a scaffold architecture with defined porosity improves cell viability, proliferation, and migration [15, 16]. Comparing the two types of scaffolds, the porous cell-laden scaffold exhibits over 30% greater vitality [17]. Cell viability and proliferation due to the interactions between cells and their substrates are significantly influenced by the swelling rate and associated pore size[18]. However, a higher swelling ratio in a short period of time will accelerate pore closure[19] and ultimately decrease the scaffold's geometric fidelity during the incubation period[20]. Therefore, the analysis of shape fidelity such as swelling rate of extruded filaments, pore sizes, and rate of material left in various time interval during incubation in perfusion bioreactor is critical. The main focus of this paper is analyzing the rate of pore closure due to the fluid flow resulting various swelling rates [21] of any provided scaffolds with defined or distorted architectures. Since, the variety of properties (such as viscosity, pH) of materials and process parameters (such as nozzle size, applied pressure, print speed) can create defined or distorted scaffold architectures [22, 23], user can get various scaffolds at post-printing stage ready to incubate in bioreactor. To demonstrate the impact of fluid flow, we fabricated scaffolds following a 0^0-90^0 deposition pattern with 8% Alginate, 4% Alginate-4% Carboxymethyl Cellulose (CMC), and 2% Alginate-6% CMC incubated, allowing a constant fluid flow for various periods such as 1, 2, 4, and 8 hours. The base color of the three materials is transparent, food coloring was added to all materials to increase visibility and appearance. The change of scaffolds fabricated with multiple material compositions was determined in terms of swelling rate, i.e., change of filament width, and material diffusion, i.e., comparison of dry material weight before and after incubation. This comparative study can assist in application-based materials selection suitable for incubating in a perfusion bioreactor.

2. MATERIALS AND METHODS

2.1 Hydrogel preparation and 3D printing of scaffolds

Three compositions such as 8% alginate (alginic acid sodium salt from brown algae) with medium viscosity (viscosity ≥2000 cps of 2% in water), 4% alginate and 4% Carboxymethyl Cellulose (CMC) (pH: 6.80) (Sigma-Aldrich, St. Louis, MO, USA), and 2% Alginate and 6% CMC were prepared using our protocol used in our earlier work [24]. We define them as A_8, A_4C_4, and A_2C_6 where numbers represent the weight percentage of solid content of each material used.

Rheological properties such as flow behavior was determined by a rotational rheometer (MCR 102, Anton Paar, Graz, Austria). A flat parallel plate geometry with a diameter of 25.0 mm and plate-plate gap of 1.0 mm was used to measure all data under the room temperature (25°C). Viscosity was determined at a range of 0.1 to 100 s^{-1} shear rate and the shear thinning parameters (n, K) were determined fitting a curve using the Power-Law ($\eta = K\dot{\gamma}^{n-1}$) where η and $\dot{\gamma}$ are viscosity and shear rate respectively.

Prepared hydrogels a was placed on the Peltier module before starting the experiments. Room temperature was considered to conduct the rheological tests having an intention of using the same condition during our extrusion process to facilitate the quick gelation of the deposited filament [25].

We used an extrusion-based 3D printer, BioX (CELLINK, Boston, MA) to release biomaterials layer-upon-layer and build scaffolds. Prepared hydrogels were loaded into 3.0 ml disposable barrel and released pneumatically on a building plat. We printed circular scaffolds (n=3) with 12 mm diameter and square scaffold (n=3) with 12 mm x 12 mm having a build height of 0.75 mm. The infill density for scaffolds was 7%. Various printing parameters such as nozzle diameter 250µm, print speed 5 mms^{-1}, layer height 0.25mm, and applied pressure 118-120 kPa were used to control the deposition rate of the hydrogels. These parameters were chosen to increase printability and pore size. The images of the deposited hydrogels and pore geometries at the same location were captured using the CK Olympus bright field microscope [26]. Rhino 6.0, a Computer-Aided Design (CAD) software, was used to design and define the vectorized toolpath of a scaffold. Slicer (https://www.slicer.org), a G-code generating program, was used to create a 3D printer-compatible file with the toolpath coordinates and all the process parameters needed to build the scaffolds. We confirmed the partial physical cross-link of the fabricated scaffold by spraying 4% (w/v) $CaCl_2$.

2.2 Bioreactor setup and tests

The Arduino controls various components around the bioreactor including solenoid pinch valves, micro vacuums, and liquid level sensors. The Arduino is connected to a power supply, micro stepper driver, and a circuit on a breadboard which allows for lower signals to be converted into higher voltages. Four output pins are connected to the microcontroller along with one input pin. The code runs on a main loop for a certain amount of time when tank 1 is full. The flow rate for fluid used was 5ml/min. If tank one is low, there will be a filling loop prior to the main loop based on the input of the liquid level sensor. After the main loop is finished, there is a waste loop that is performed to cycle away any unwanted cell waste. There are solenoid pinch valves between tank two and tank one, and between tank two and tank one to ensure medium cannot flow when it is not supposed to. The pinch valves are normally closed, the valve between tank two and tank one is running off 12V DC from the power supply. The pinch valve between tank two and the waste tank is also normally closed but runs off 24V DC from the power supply. The Arduino is powered by 5V DC from the power supply which also powers both Micro vacuums. This system allows for closed loop operation of the Bioreactor.

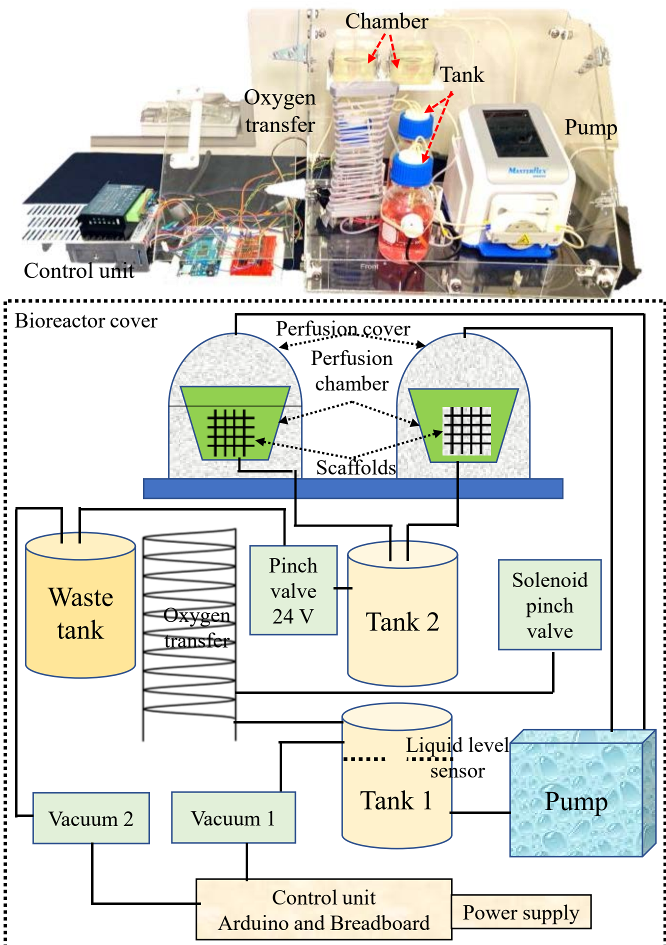

FIGURE 1: A prototype setup along with a schematic diagram of our designed perfusion bioreactor. After completing the final setup, we will place it directly into the incubator.

This research demands good amount of time and resources that drove us to collect most of the data one time. For demonstration purpose, we collected the data for swelling rate twice of A_4C_4 for 1, 2, 3, and 4 hours to analyze the repeatability which did not show a significant difference, meaning those data showed a repetition. This research is still on-going and in future, we will collect each data at least three times to demonstrate the repeatability. We used a statistical software, Origin Pro 2021b (Northampton, MA, USA) to generate the graphs.

3. RESULTS AND DISCUSSION

3.1 Flow behavior of hydrogel used

From Figure 2, it is clear that all three compositions showed a shear thinning behavior because of their decreasing trend of viscosity (η) with respect to shear rate ($\dot{\gamma}$). The K values (viscosity value at 1.0 s^{-1} shear rate) of A_8, A_4C_4, and A_2C_6 are 11031, 21209, and 26059 mPa.S respectively which indicates that the amount of viscosity was CMC-dependent. Therefore, it is expected that scaffolds fabricated with higher percentage of CMC will preserve the shape fidelity.

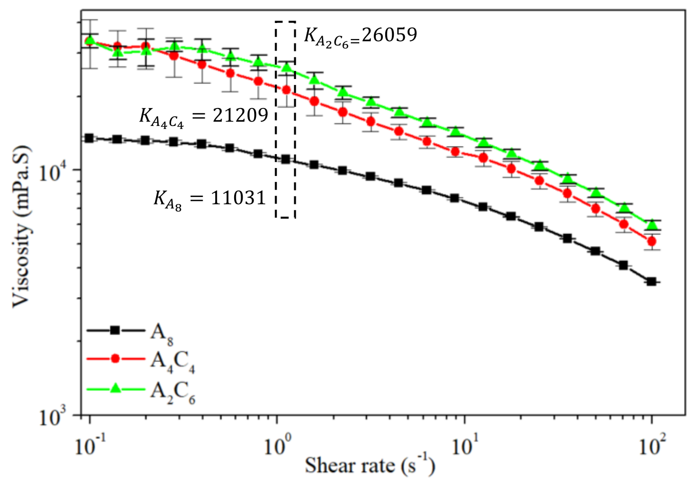

FIGURE 2: FLOW BEHAVIOR OF A_8, A_4C_4, and A_2C_6 USED IN THIS PAPER.

3.2 Analysis of pore size of scaffolds after printing and crosslinking

Scaffolds with circular geometry were fabricated using all three compositions of A_8, A_4C_4, and A_2C_6 (after submerging into the bioreactor chamber) as shown in Figure 3 and Figure 4. The printed parts immediately after coming out the printer have the texture of a liquid gel. After crosslinking the hydrogel for 7 minutes the scaffolds gain much needed strength. The crosslinking allows the scaffold to be moved, measured on a scale, observed under the microscope, and placed in the bioreactor. Pore sizes were measured at t=0, t=1.0 and t=2.0 min after printing. Figures 3 and 4 represent a clear intention of pore close with time. The rate of pore closure of scaffolds fabricated with **A**$_8$, A_4C_4, and A_2C_6 are 55%, 72%, and 69% respectively after 1.0 min of fabrication compared to the pore size right after scaffold fabrication.

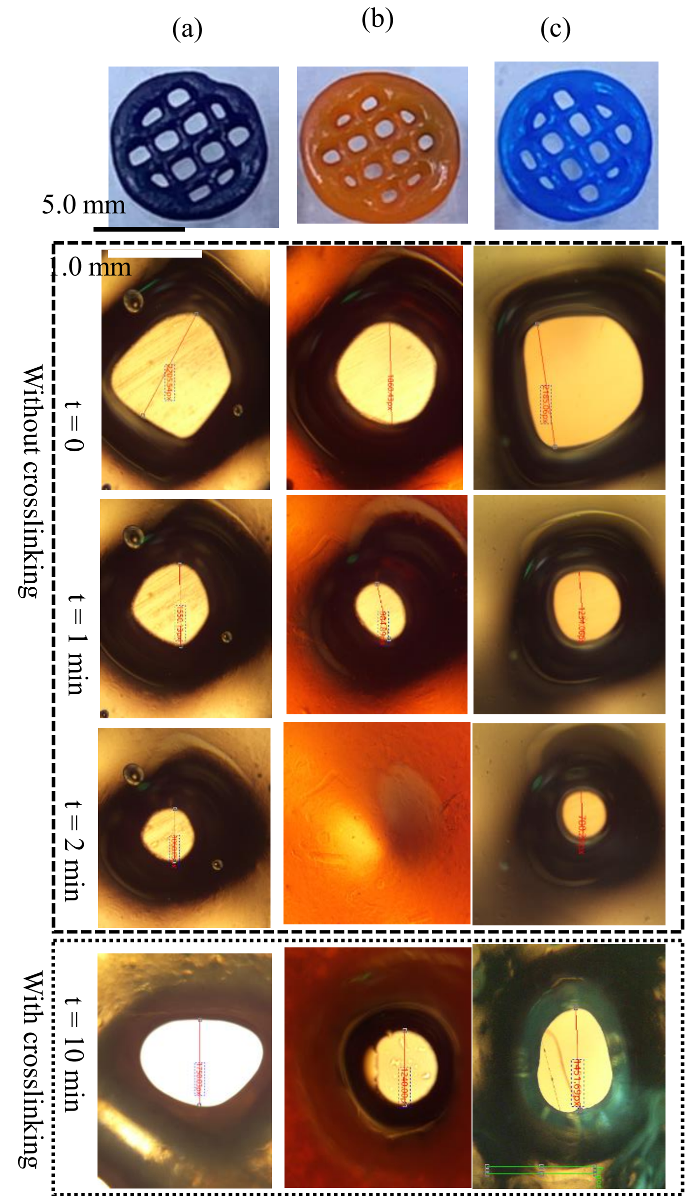

FIGURE 3: FABRICATED SCAFFOLDS AND PORE GEOMETRIES OF THOSE SCAFFOLDS FABRICATED WITH (A) A_2C_6 (B) A_4C_4 AND (C) A_8 AT DIFFERENT TIME PERIODS AFTER PRINTING AND CROSSLINKING.

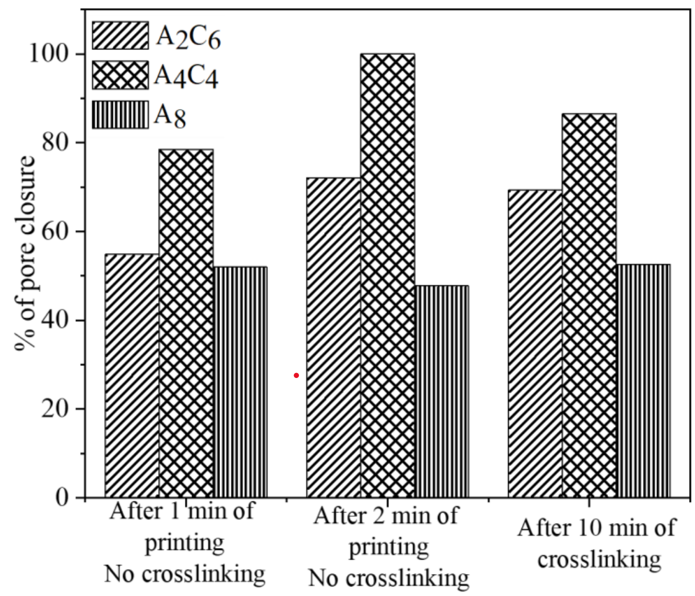

FIGURE 4: FABRICATED SCAFFOLDS AND PORE GEOMETRIES OF THOSE SCAFFOLDS FABRICATED WITH (A) A_2C_6 (B) A_4C_4 AND (C) A_8 AT DIFFERENT TIME AFTER PRINTING AND CROSSLINKING.

Since A_2C_6 has higher viscosity, scaffold fabricated with this composition showed less pore closure rate compared to the scaffolds fabricated with two other compositions. A set of scaffolds were crosslinked right after the fabrication and the rate of pore closure was analyzed with the microscopic view of pore. The pore closure rates after 10 minutes of crosslinking were 52%, 70%, and 50% respectively. Even, A_8 has lower viscosity compared to A_2C_8 and A_4C_4, the rate of pore closure compared to A_2C_8 and A_4C_4 is lower at crosslinked situation. Because A_8 is more responsive to $CaCl_2$ than A_2C_8 and A_4C_4 due to the higher percentage of alginate. This observation supports with our earlier published papers where we presented the statistically significant differences of swelling rate and pore closure of similar material compositions [24, 27].

3.3 Analysis of swelling rate into the bioreactor chamber

After crosslinking, scaffolds were placed into the bioreactor chamber, and water was flown through the scaffolds as shown in Figure 5. It is clear from Figure 6(a) that, A_2C_6 was not a viable option for perfusion. As seen in Figure 6(a), the biomaterial departed from its initial structure after 1 hour and lost all porosity after 2 hours and finally 3- and 4-hour tests were destroyed due to perfusion. The scaffold was unable to retain more than half of the original material. Also, to be noted, the scaffolds endured severe swelling at 3- and 4-hour testing during perfusion as shown in Figure 7(a). At 4-hour testing, we were barely able to capture the filament width that resulted around 200% swelling rate. This trend of swelling matched with the amount of material retain i.e., 35% and 20% after 3.0 and 4 hours respectively as shown in Figure 7(b).

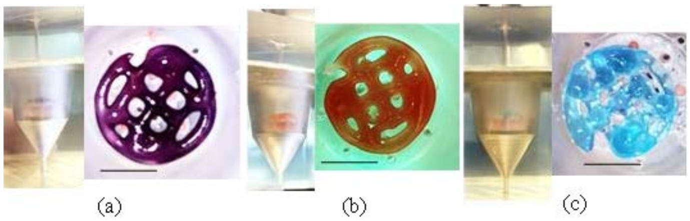

FIGURE 5: CROSSLINKED 3D PRINTED SCAFFOLDS FABRICATED WITH (a) A_2C_6 (b) A_4C_4, AND (c) A_8 PLACED INTO THE PERFUSION CHAMBER BEFORE STARTING THE FLUID FLOW. SCALE BAR = 5.00 MM.

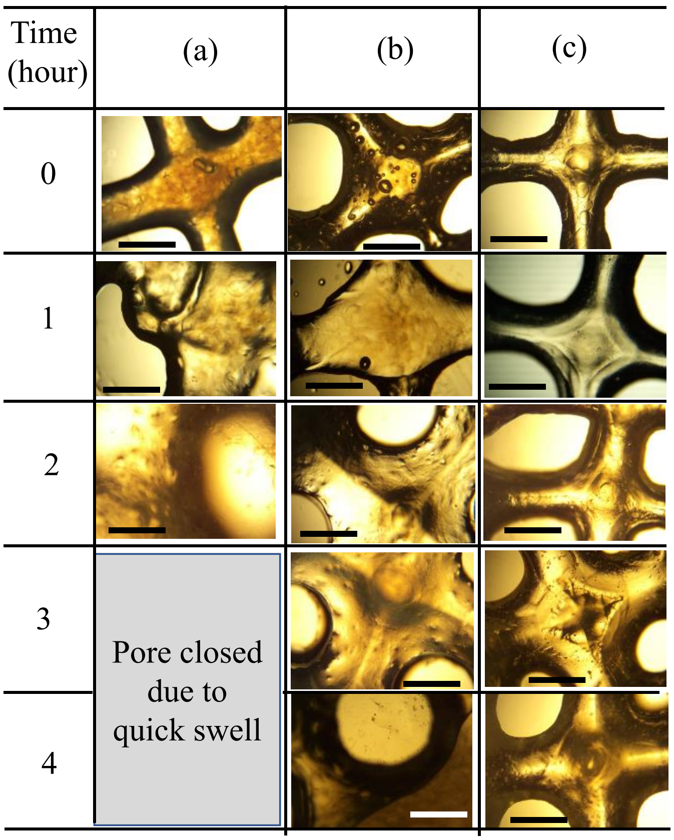

FIGURE 6: FILAMENT SWELLING AT 1-, 2-, 3-, AND 4-HOURS INCUBATION TIME FABRICATED WITH (a) A_2C_6 (b) A_4C_4, AND (c) A_8. SCALE BAR = 1MM.

Systematic process parameters selection such as medium flow rate, percentage of crosslinker and crosslinking time, and size of filament width can help achieve acceptable swelling rate for scaffold fabricated with A_2C_6.

A_4C_4 was a viable option to incubate into the perfusion bioreactor. Microscopic observation indicates that all tests held structures up to 8 hours of experiment. Results up to 4 hours were included for comparison purpose as shown in Figure 6 and Figure 7. The tests swelled at a consistent rate throughout all tests as shown in Figure 6(b) and Figure 7 ensuring structure. Prints were left with over 54% material in all tests as shown in cells as shown in Figure 7(b). In our prior work, we demonstrated around 86% cell viability encapsulated into A_4C_4 [24]. Therefore, we expect this material has the capacity to incubate even in our perfusion bioreactor encapsulating living cells due to its positive swelling rates, low degradation percentages, and its ability to hold structure.

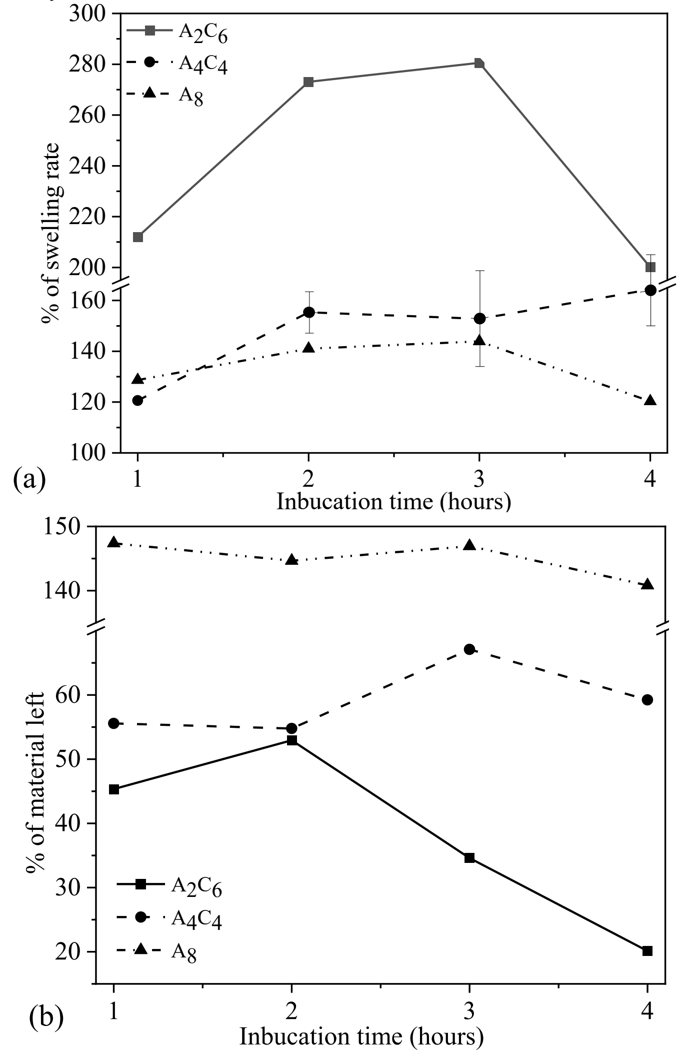

FIGURE 7: (a) % OF SWELLING RATE AND (b) % OF MATERIAL LEFT FABRICATED WITH A_2C_6, A_4C_4, AND (C) A_8.

A_8 is the most rigid material that was tested. It was apparent that crosslinking the scaffold fabricated with A_8 made instantly rigid and durable. Uniform pore geometry was observed microscopically as shown in Figure 6(c). Higher percentage of crosslinking did not allow the scaffold to absorb enough water to swell it positively. That trend supported the amount of material left even after 4 hours of incubation. The % material after perfusion came out at a higher rate than the amount of material in the scaffolds. We suspect that the amount of time we allowed (24 hours) the scaffold was not enough to completely dry. Since, it has more crosslinking bond, water may get less access to come out and the scaffold get dried. A new set of experiment was conducted for square-shaped scaffold. The swelling rate and percentage of material lost after 1, 2, 3, and 4 hours of incubation were determined. Same pore was captured to analyze the swelling rate. After completing each period of incubation (1, 2, 3, and 4 hours), material was dried to determine the percentage of material lost. Printed, submerged, and dried scaffold along with the pore geometry after the incubation of each period are shown in Figure 8.

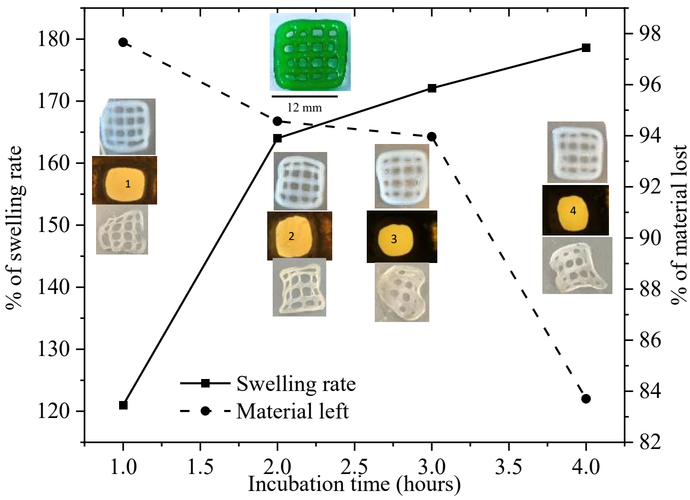

FIGURE 8: % of swelling rate and % of material lost fabricated with A_4C_4. Scaffold with green color was just after the printing. Then we crosslinked the scaffold and incubated for 1, 2, 3, and 4 hours. The geometry of pore after swelling was captured by microscope. Finally we dried the scaffolds after 1, 2, 3, and 4 hours of incubation to determine the percentage of material lost due to swelling.

4. CONCLUSION

This paper outlined the importance of shape fidelity analysis such as swelling rate of extruded filaments, pore sizes, and rate of material left in various time interval during incubation in perfusion bioreactor is critical. We mimicked the fluid flow through the scaffolds fabricated with various material compositions having different viscosities we will fabricate encapsulating cells in future to explore the response. We clearly identified the different swelling behavior of materials having varying viscosities under dynamic fluid flow that can help select right material type to incubate in perfusion bioreactor. Experiments also helped determine material diffusion after incubation. In future we will use other types of material compositions crosslinking them with various time periods to analyze the swelling behavior and material diffusion rate. This comparative study can assist in application-based materials selection suitable for incubating in a perfusion bioreactor.

ACKNOWLEDGEMENTS

Research was supported by New Hampshire-EPSCoR through BioMade Award #1757371 from National Science Foundation and New Hampshire-INBRE through an Institutional Development Award (IDeA), P20GM103506, from the National Institute of General Medical Sciences of the NIH.

REFERENCES

[1] C. Zhang *et al.*, "3D culture technologies of cancer stem cells: promising ex vivo tumor models," *Journal of tissue engineering,* vol. 11, p. 2041731420933407, 2020.

[2] S. V. Murphy and A. Atala, "3D bioprinting of tissues and organs," *Nature biotechnology,* vol. 32, no. 8, pp. 773-785, 2014.

[3] S. M. Mueller, S. Mizuno, L. C. Gerstenfeld, and J. Glowacki, "Medium Perfusion Enhances Osteogenesis by Murine Osteosarcoma Cells in Three-Dimensional Collagen Sponges," *Journal of Bone and Mineral Research,* vol. 14, no. 12, pp. 2118-2126, 1999.

[4] G. N. Bancroft, V. I. Sikavitsas, and A. G. Mikos, "Technical note: Design of a flow perfusion bioreactor system for bone tissue-engineering applications," *Tissue engineering,* vol. 9, no. 3, pp. 549-554, 2003.

[5] F. W. Janssen, J. Oostra, A. van Oorschot, and C. A. van Blitterswijk, "A perfusion bioreactor system capable of producing clinically relevant volumes of tissue-engineered bone: in vivo bone formation showing proof of concept," *Biomaterials,* vol. 27, no. 3, pp. 315-323, 2006.

[6] A. Abbatiello and M. A. Habib, "Development of an In-House Customized Perfusion-Based Bioreactor for 3D Cell Culture," in *International Manufacturing Science and Engineering Conference*, 2022, vol. 85802: American Society of Mechanical Engineers, p. V001T01A016.

[7] A. M. Leferink, Y.-C. Chng, C. A. Van Blitterswijk, and L. Moroni, "Distribution and viability of fetal and adult human bone marrow stromal cells in a biaxial rotating vessel bioreactor after seeding on polymeric 3D additive manufactured scaffolds," *Frontiers in bioengineering and biotechnology,* vol. 3, p. 169, 2015.

[8] S. Grogan, F. Rieser, V. Winkelmann, S. Berardi, and P. Mainil-Varlet, "A static, closed and scaffold-free bioreactor system that permits chondrogenesis in vitro," *Osteoarthritis and cartilage,* vol. 11, no. 6, pp. 403-411, 2003.

[9] W. Zhou *et al.*, "Multifunctional bioreactor system for human intestine tissues," *ACS Biomaterials Science & Engineering,* vol. 4, no. 1, pp. 231-239, 2018.

[10] D. Mitra, J. Whitehead, O. W. Yasui, and J. K. Leach, "Bioreactor culture duration of engineered constructs influences bone formation by mesenchymal stem cells," *Biomaterials,* vol. 146, pp. 29-39, 2017.

[11] K. Sampson *et al.*, "Cultivation of hierarchical 3D scaffolds inside a perfusion bioreactor: scaffold design and finite-element analysis of fluid flow," *SN Applied Sciences,* vol. 3, no. 12, pp. 1-17, 2021.

[12] R. Visone, G. Talò, S. Lopa, M. Rasponi, and M. Moretti, "Enhancing all-in-one bioreactors by

combining interstitial perfusion, electrical stimulation, on-line monitoring and testing within a single chamber for cardiac constructs," *Scientific reports,* vol. 8, no. 1, pp. 1-13, 2018.

[13] M. Panek *et al.*, "Bone tissue engineering in a perfusion bioreactor using dexamethasone-loaded peptide hydrogel," *Materials,* vol. 12, no. 6, p. 919, 2019.

[14] J. A. S. Neiman *et al.*, "Photopatterning of hydrogel scaffolds coupled to filter materials using stereolithography for perfused 3D culture of hepatocytes," *Biotechnology and bioengineering,* vol. 112, no. 4, pp. 777-787, 2015.

[15] C. M. Murphy, M. G. Haugh, and F. J. O'Brien, "The effect of mean pore size on cell attachment, proliferation and migration in collagen–glycosaminoglycan scaffolds for bone tissue engineering," *Biomaterials,* vol. 31, no. 3, pp. 461-466, 2010.

[16] R. A. Perez and G. Mestres, "Role of pore size and morphology in musculo-skeletal tissue regeneration," *Materials Science and Engineering: C,* vol. 61, pp. 922-939, 2016.

[17] R. Gaetani *et al.*, "Cardiac tissue engineering using tissue printing technology and human cardiac progenitor cells," *Biomaterials,* vol. 33, no. 6, pp. 1782-1790, 2012.

[18] C. E. Vorwald, T. Gonzalez-Fernandez, S. Joshee, P. Sikorski, and J. K. Leach, "Tunable fibrin-alginate interpenetrating network hydrogels to support cell spreading and network formation," *Acta biomaterialia,* vol. 108, pp. 142-152, 2020.

[19] S. Grabska-Zielińska, A. Sionkowska, K. Reczyńska, and E. Pamuła, "Physico-chemical characterization and biological tests of collagen/silk fibroin/chitosan scaffolds cross-linked by dialdehyde starch," *Polymers,* vol. 12, no. 2, p. 372, 2020.

[20] S. Sultan and A. P. Mathew, "3D printed scaffolds with gradient porosity based on a cellulose nanocrystal hydrogel," *Nanoscale,* vol. 10, no. 9, pp. 4421-4431, 2018.

[21] G. Bai and A. Suzuki, "Effects of continuous water flow on the swelling properties of polyelectrolyte hydrogels," *The European Physical Journal E,* vol. 14, pp. 107-113, 2004.

[22] N. Diamantides *et al.*, "Correlating rheological properties and printability of collagen bioinks: the effects of riboflavin photocrosslinking and pH," *Biofabrication,* vol. 9, no. 3, p. 034102, 2017.

[23] S. Kyle, Z. M. Jessop, A. Al-Sabah, and I. S. Whitaker, "'Printability'of Candidate Biomaterials for Extrusion Based 3D Printing: State-of-the-Art," *Advanced healthcare materials,* vol. 6, no. 16, p. 1700264, 2017.

[24] A. Habib, V. Sathish, S. Mallik, and B. Khoda, "3D printability of alginate-carboxymethyl cellulose hydrogel," *Materials,* vol. 11, no. 3, p. 454, 2018.

[25] L. Ouyang, R. Yao, Y. Zhao, and W. Sun, "Effect of bioink properties on printability and cell viability for 3D bioplotting of embryonic stem cells," *Biofabrication,* vol. 8, no. 3, p. 035020, 2016.

[26] R. S. Kumar V, Cutkosky M, Dutta D, " Representation and processing heterogeneous objects for solid freeform fabrication," ed. Sixth IFIP WG 5.2 International Workshop on Geometric Modelling: Fundamentals and Applications, Tokyo, Japan, The University of Tokyo, 1998.

[27] C. Nelson, S. Tuladhar, L. Launen, and M. Habib, "3D Bio-Printability of Hybrid Pre-Crosslinked Hydrogels," *International Journal of Molecular Sciences,* vol. 22, no. 24, p. 13481, 2021.

(1)

.